Direct Observation of a Surface Induced Disordering Process in Magnetic Nanoparticles

András Kovács,[1,*] Kazuhisa Sato,[2] Vlado K. Lazarov,[1,†] Pedro L. Galindo,[3] Toyohiko J. Konno,[2] and Yoshihiko Hirotsu[4]

[1]*Department of Materials, University of Oxford, Parks Road, OX1 3PH Oxford, United Kingdom*
[2]*Institute for Materials Research, Tohoku University, 2-1-1 Katahira, Sendai 980-8577, Japan*
[3]*Departamento de Lenguajes y Sistemas Informáticos, CASEM, Universidad de Cádiz, Polígono Rio San Pedro s/n. 11510, Puerto Real, Cadiz, Spain*
[4]*The Institute of Scientific and Industrial Research, Osaka University, 8-1 Mihogaoka, Ibaraki 5670047, Japan*

(Received 23 March 2009; revised manuscript received 14 July 2009; published 11 September 2009)

We present experimental evidence of surface induced disordering at magnetic FeCoPd nanoparticles during the $L1_0$-$A1$ phase transition using high-resolution aberration-corrected electron microscopy and strain mapping. *In situ* electron diffraction studies show a narrow temperature range of fully ordered $L1_0$ structure. The order-disorder transition is size dependent and induces strong lattice deformation in outer part of the nanocrystals. The formation of unusually large strain of 20% is discussed in terms of core-shell structure formation with surface disordered layer and ordered core.

DOI: 10.1103/PhysRevLett.103.115703 PACS numbers: 64.70.Nd, 68.37.Lp, 75.75.+a

Nanoparticles (NPs) have unique properties because they are finite small objects with large surface-volume ratio, which makes them suitable for novel functional applications. NPs that possess magnetic properties offer exciting new opportunities for applications ranging from biomedical purposes [1,2] to magnetic recording [3]. The type of magnetism often varies depending on the size and structure of the crystals. For example, magnetic particles of the FePt family are superparamagnetic below a critical size [4], than show soft ferromagnetism in disordered state, and presence of strong magnetic anisotropy when the structure is ordered. The order (tetragonal, $L1_0$) disorder (cubic, $A1$) transformation is size dependent and the results of theoretical modeling suggest that the disordering process is surface related [5,6].

The attractive magnetic properties [7,8] of the $L1_0$ structure originate from their ordered crystal structure (CuAu (I) type) where typically the Fe(Co) and Pd(Pt) atoms alternate along the [001] direction which is the magnetic easy axis. The large magnetic anisotropy energy of the order of $\sim 10^7$ erg/cm^3 (Refs. [7,8]) allows the nm-sized particles to withstand thermal fluctuations of the direction of magnetization which is vital for future high density magnetic memories [3]. In general, the chemical ordering of the $L1_0$ structure is obtained by annealing at moderately high temperature and the magnetic anisotropy strongly correlates with the long-range order parameter of the $L1_0$ structure [9]. The random distribution of the atoms results in a disordered face centered cubic (fcc) structure and soft ferromagnetic properties. The order ($L1_0$)-disorder ($A1$) structural transformation phenomenon of nm-sized particles is not well understood. Lipowsky's work [10] on bulk first-order phase transition showed that ''a layer of the disordered phase intervenes between the free surface and ordered bulk.'' Recent Monte Carlo simulations [6,11] of $L1_0$ order-disorder transition suggest surface induced disordering mechanism of nm-sized crystals with a segregation process. The surface segregation has been shown in work of Wang and co-workers [12]; they report the lattice expansion of the surface shells of disordered fcc FePt icosahedral NPs caused likely by the preferential Pt segregation.

In this Letter, we show experimentally, for the first time that disordering process in $L1_0$ NPs starts by the formation of surface disordered layers. The surface volume increase due to the disordered layer formation, result in formation of significant strain that heavily distort the structure of the particles. The observation and quantification of surface disordered layer formation and the elastic strain in nanoparticles is challenging because of the very small amount of material and the limitations of the experimental techniques. Recent developments in high resolution transmission electron microscopy (HRTEM) such as spherical aberration (C_s) corrected TEM [13,14] gives the advantage of atomic imaging as it provides a better resolution with enhanced image contrast and most importantly absence of delocalization artifacts [15]. In addition, the capability for precise determination of atomic positions in C_s-corrected HRTEM images allows precise quantification of the strain of the individual NPs by using numerical image-processing techniques [16,17]. We investigate the ordered $L1_0$ phase formation and the effect of order-disorder phase transformation processes on functional properties of Co-doped Fe-Pd particles.

Pd-Co-Fe particles were prepared by sequential deposition in an UHV system at 473 K on NaCl (001) substrates. As a result, a composite structure of seed fcc Pd and top alloyed body-centered cubic (bcc) CoFe were formed with epitaxial relationship of $[001]_{FeCo} \parallel [001]_{Pd}$, $(110)_{FeCo} \parallel (100)_{Pd}$. A 10-nm-thick amorphous Al_2O_3 layer was deposited on the surface to prevent the particles from the oxidation and stabilize them in separated condi-

tion. The layer was immersed in distilled water and mounted on Mo grids. A small amount of Co can dissolve in the $L1_0$-FePd lattice by replacing the Fe sites leading to an increased magnetic moment of the system [18,19]. Size distribution of the particles shows a log-normal distribution with a mean size of 10.5 nm and shape parameter of 0.14. Chemical composition of the particles was determined by energy dispersive x-ray spectroscopy as $Fe_{38}Co_6Pd_{56}$.

We followed the $L1_0$ phase formation by the appearance of the characteristic 110 superlattice reflections as a function of temperature in the selected area electron diffraction (SAED) patterns, as shown in Fig. 1(a). For the TEM analysis, we used a JEM-3000F (JEOL) microscope. Qualitative information regarding to formation of the tetragonal ordered structure is obtained using the intensity ratio of characteristic 110 superlattice and 220 fundamental reflections (I_{110}/I_{220}) measured in SAED patterns [Fig. 1(a)]. Multislice simulation of diffraction intensities shows that the intensity change of 220 reflections during the phase transformation from the disorder Fe-Co-Pd structure to the $L1_0$ ordered one is negligible (~0.5%). The increasing I_{110}/I_{220} ratio [Fig. 1(a)] during the annealing process consistently shows the evolution of $L1_0$ ordering in NPs up to 873 K due to the fast interdiffusion of Pd and Co-Fe atoms. Conventional HRTEM analysis of NPs at 873 K confirmed [Fig. 1(b)] the single crystal $L1_0$ phase formation in NPs with tetragonal c axis (magnetic easy axis) perpendicular to the image plane. The particles are faceted and have octahedral shape with truncated edges. The HRTEM images do not reveal any structural distortion of the NPs at this temperature. Increasing the temperature above 873 K results in the gradual decrease of I_{110}/I_{220} ratio [Fig. 1(a)] indicating the degradation of the $L1_0$ phase. The weakening of 110 reflections relates to the start of order-disorder transformation process in $L1_0$-FeCoPd NPs. The disordering process is accelerated above 973 K reflected in a rapid decrease of the I_{110}/I_{220} ratio; however, the ordered reflections in SAED patterns are still observable at 1023 K [Fig. 1(a)]. The observed structural changes in NPs during annealing process strongly affect their functional properties. We followed the magnetic properties of NPs by measuring the out-of-plane coercivity at different temperatures [Fig. 1(a)]. Magnetic properties were measured using a Quantum Design SQUID magnetometer at room temperature and at 10 K in perpendicular and parallel to the substrate surface. The coercivity change strongly correlates with the structural changes of NPs with the maximum coercivity of 3480 Oe at room temperature after the annealing at 873 K [Fig. 1(a)].

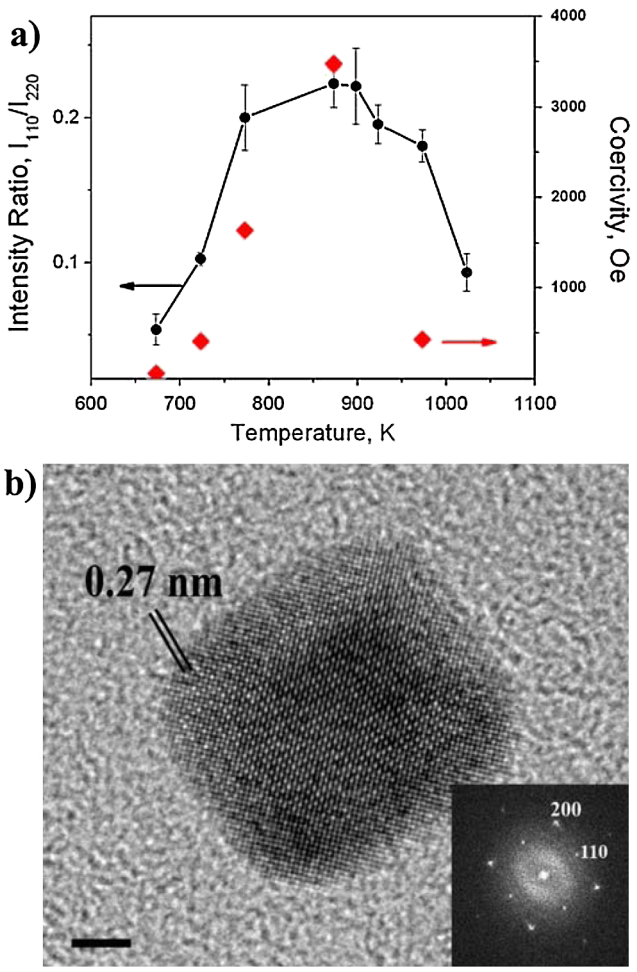

FIG. 1 (color online). Ordering and disordering process of NPs. (a) Intensity ratio of I_{110}/I_{220} and out-of plane magnetic coercivity as a function of the annealing temperature. The I_{110}/I_{220} ratio determined in electron diffraction patterns. Coercivity is measured at room temperature. (b) Conventional HRTEM image of an $L1_0$ ordered NP recorded at 873 K. 110 reflections in the diffractogram (inset) and the large (0.27 nm) lattice fringes of 110 planes in HRTEM image confirm the $L1_0$ ordered state. The scale bar is 2 nm.

To examine the structure of individual NPs after the annealing, we have carried out nanobeam diffraction (NBD) analysis (Fig. 2) at room temperature followed

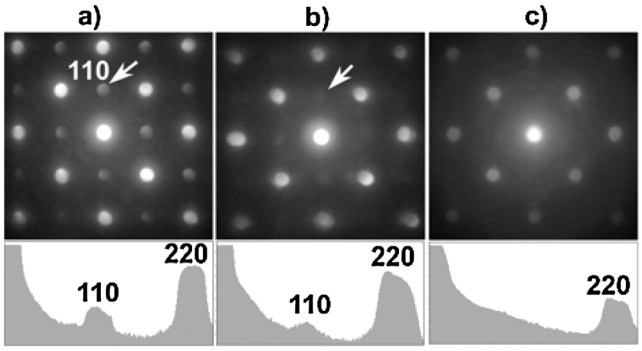

FIG. 2. Size dependence of $L1_0$-$A1$ phase transformation. NBD patterns of particles with diameter of 13 (a), 9 (b), and 6 nm (c). Arrows indicate the 110 superlattice reflection of the $L1_0$ phase. The intensity line scans of 110 and 220 reflections show the disappearance of ordered reflection with decreasing the size.

the annealing. Particles larger than 10 nm show the characteristic 110 superlattice reflections of the $L1_0$ structure in NBD pattern [Fig. 2(a)] indicating that the. Close examination of NBD pattern from the particles smaller than 10 nm show a weak ordered reflection [Fig. 2(b)]. No sign of ordered structure is present for the particles smaller than 6 nm [Fig. 2(c)]. The inset intensity line scans along the 110 and 220 reflections confirm the different order state of NPs with respect to their size. The NBD and HRTEM image analyses (not shown) showed that the disordering process is size dependent and amplified for particles with diameter less than 10 nm.

We now focus on the mechanism of $L1_0$-$A1$ phase transformation. We have used a C_s-corrected HRTEM imaging to reveal the nature of disordering process in nanoparticles, by measuring precisely their atomic column positions. The imaging is carried out at room temperature of the *in situ* annealed sample. For the C_s-corrected TEM analysis, Titan 80–300 (FEI) instrument was used. TEM image acquisition was performed with a small overfocus and a negative C_s values ($C_s = -9.6$ μm). Multislice image simulations confirm that these image conditions result in bright contrast of atomic columns in HRTEM images [Fig. 3(a) inset]. The HRTEM image and the corresponding digital diffractogram [Fig. 3(a) inset] clearly show the presence of the $L1_0$ ordered structure in a large NP, while less ordered

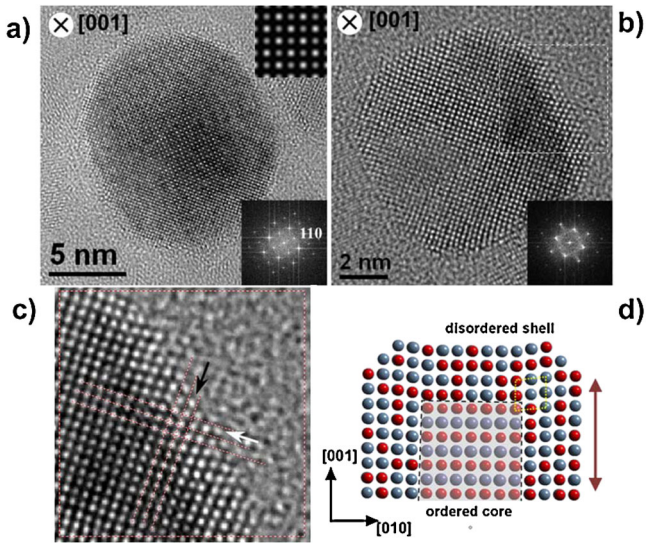

FIG. 3 (color online). Aberration-corrected HRTEM images of *in situ* annealed particles. (a) The image recorded from a large particle (11.8×13.9 nm) shows $L1_0$ ordered structure with straight atomic planes. An enlarged simulated HRTEM image of the $L1_0$ structure is inserted. (b) In smaller (8.5×8.5 nm) NPs the edge atomic columns are heavily distorted by the formation of the surface disordered layer. (c) Typically the last 4–5 atomic columns are displaced. Dashed lines help to guide the eyes. (d) Schematic cross section shows how the SID forms an ordered core-disordered shell structure with significant distortion at the edges.

state and very strong lattice distortion is found in the NPs with sizes smaller than 9 nm. To show the distortion of the lattice clearly, a selected area of the edge of the 8.5 nm-sized NP [Fig. 3(b)] is enlarged and presented in Fig. 3(c). The atomic planes at the edge of the particle are displaced from their bulk-core cubic arrangement (labeled with red doted lines) in both directions [Figs. 3(b) and 3(c)]. We have found that such distorted surface planes are typical for annealed NPs in range of diameters from 6 to 9 nm. In this size range of the NPs, the larger ones show ordered structure only at their center area. The last four atomic columns are misplaced for 0.12, 0.09, 0.06, and 0.03 nm with respect to their bulk-core like positions as shown in Fig. 3(c) for (100) type of atomic plane. Similar values are obtained for (010) type of planes (marked by black arrow), which is a remarkable distortion for the structure.

The distorted surface structure of the NP can be explained by the formation of the surface disordered layers. The disordered ($A1$) Pd-Co-Fe is an fcc while the ordered $L1_0$ is a tetragonal structure with smaller c lattice constant ($a_{L1o} = 0.383 \pm 0.002$ nm, $c_{L1o} = 0.375 \pm 0.002$ nm). By the $L1_0$-$A1$ phase transformation, the (001) planes distance is being elongated along the c axis in order to form the $A1$ structure. Since the process starts from the surface, number of the unit cells along the [001] direction from the surface layers at side [Fig. 3(d) arrow] that undergo phase transformations is significantly bigger than the number of unit cell on the top and bottom of NPs (along [001]). This process produces unequal strain distribution, which results in a rhombohedral deformation of the lattice of the surface layers, as outlined by the schematic cross section of a surface disordered particle in Fig. 3(d). The interface between the ordered and disordered part of the particle likely has a diffuse transition character similarly to Au-Cu nanoparticles [20].

The significant volume changes at the particle sides results in a lattice distortion that introduces a subtle strain to the particles. We mapped the strain by using peak pairs algorithm [17] (PPA). For the strain analyses, we used the same particles that are shown in Fig. 3. Predefined directions (x and y) were chosen to be parallel and perpendicular to the [110] direction, as indicated in Fig. 4. Strain analysis shows compression distortions (e_{xx}, $e_{yy} = 0.2 \pm 0.1$) at the edges of small particle, while for large ones, strain values are negligible (e_{xx}, $e_{yy} = 0.0 \pm 0.05$). These results confirm that large strain is accumulated at the surface at the particles, within the 6–9 nm range, due to the order-disorder transition. Larger particles (bigger than 9 nm) may have a thin disordered surface layer, but that did not generate significant lattice distortion and strain.

Present experimental results indicate that the disordering process begins at the surface and then proceeds to the interior of the nanoparticles forming a disorder surface and ordered core structure of the particles for the given size distribution (and temperature). Unfortunately, the chemical

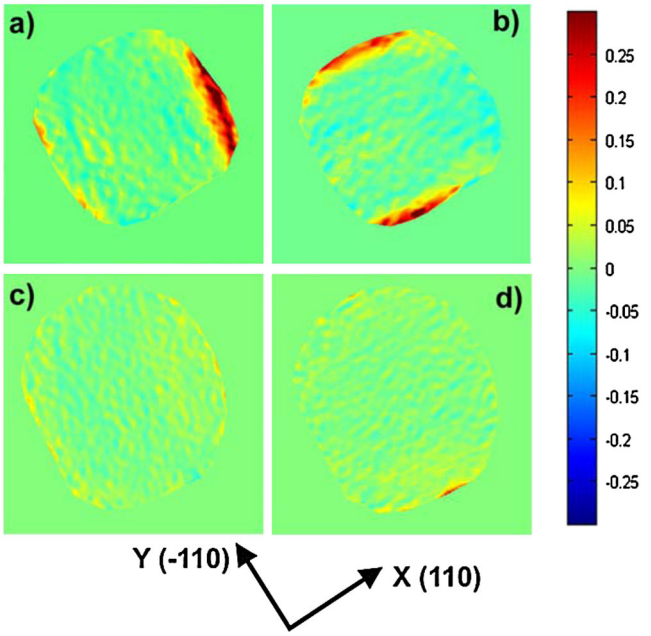

FIG. 4 (color online). Strain distribution in the NPs in Fig. 3. Strain maps of e_{xx} (a) and e_{yy} (b) of small NP show a remarkable tensile stress at the edges of the particle (a) and (b) while for large NP, strain is not present (c) and (d).

distribution of the atoms in annealed nanoparticles, which is necessary to reveal the surface composition and segregation process, is not possible from the methods used in this study. Dedicated future experiments will be necessary to reveal the extent of the surface segregation effect during the order-disorder transition.

In summary, recent advances in aberration corrected atomic imaging and the related direct measurements of strain distribution in crystalline nm-sized particles made possible direct observation of the surface induced disordering process of $L1_0$-FeCoPd particles. Disordering is size dependent phenomenon, which is more pronounced in smaller particles due to the large surface/volume ratio. The core-shell structure, resulting from order-disorder transformation, introduces significant lattice distortions and strain to the particles' surface. The magnetic properties are directly correlated to their structural changes observed during the annealing process. Our results give a new insight to $L1_0$-$A1$ phase transformation mechanism of crystalline particles that can be a general process applicable for other type of order-disorder transition of nanostructures.

A. K. on leave from Research Institute for Technical Physics and Materials Science, Budapest, Hungary. This study was supported by the Grant-in-Aid for Scientific Research (S) (No. 16106008) and by the Grant-in-Aid for Young Scientists (B) (Grant No. 19760459) from the Ministry of Education, Culture, Sports, Science and Technology, Japan, and by the Spanish MEC (TEC2005-05781-C03-02 and MAT2007-60643).

*andras.kovacs@materials.ox.ac.uk
†Present address: Department of Physics, University of York, JEOL Nanocentre, YO10 5DD York, United Kingdom.

[1] M. Lewin, N. Carlesso, C. H. Tung, X. W. Tang, D. Cory, D. T. Scadden, and R. Weissleder, Nat. Biotechnol. **18**, 410 (2000).
[2] C. B. Berry and A. S. G. Curtis, J. Phys. D **36**, R198 (2003).
[3] S. Sun, C. B. Murray, D. Weller, L. Folks, and A. Moser, Science **287**, 1989 (2000).
[4] T. Miyazaki, O. Kitakami, S. Okamoto, Y. Shimada, Z. Akase, Y. Murakami, D. Shindo, Y. K. Takahashi, and K. Hono, Phys. Rev. B **72**, 144419 (2005).
[5] R. V. Chepulskii and W. H. Butler, Phys. Rev. B **72**, 134205 (2005).
[6] B. Yang, M. Asta, O. N. Mryasov, T. J. Klemmer, and R. W. Chantrell, Acta Mater. **54**, 4201 (2006).
[7] M. R. Visokay and R. Sinclair, Appl. Phys. Lett. **66**, 1692 (1995).
[8] H. Shima, K. Oikawa, A. Fujita, K. Fukamichi, K. Ishida, and A. Sakuma, Phys. Rev. B **70**, 224408 (2004).
[9] S. Okamoto, N. Kikuchi, O. Kitakami, T. Miyazaki, Y. Shimada, and K. Fukamichi, Phys. Rev. B **66**, 024413 (2002).
[10] R. Lipowsky, Phys. Rev. Lett. **49**, 1575 (1982).
[11] M. Müller and K. Albe, Phys. Rev. B **72**, 094203 (2005).
[12] R. M. Wang, O. Dmitrieva, M. Farle, G. Dumpich, H. Q. Ye, H. Poppa, R. Kilaas, and C. Kisielowski, Phys. Rev. Lett. **100**, 017205 (2008).
[13] K. W. Urban, Science **321**, 506 (2008).
[14] C. J. D. Hetherington, S. Chang, S. Haigh, P. D. Nellist, L. C. Gontard, R. E. Dunin-Borkowski, and A. Kirkland, Microsc. Microanal. **14**, 60 (2008).
[15] H. W. Zandbergen, D. Tang, and D. Van Dyck, Ultramicroscopy **64**, 185 (1996).
[16] C. L. Johnson, E. Snoeck, M. Ezcurdia, B. Rodríguez-González, I. Pastoriza-Santos, L. M. Liz-Marzán, and M. J. Hÿtch, Nature Mater. **7**, 120 (2008).
[17] P. L. Galindo, S. Kret, A. M. Sanchez, J. Y. Laval, A. Yáñez, J. Pizarro, E. Guerrero, T. Ben, and S. I. Molina, Ultramicroscopy **107**, 1186 (2007).
[18] K. Noma, M. Matsuoka, H. Kanai, Y. Uehara, K. Nomura, and N. Awaji, IEEE Trans. Magn. **42**, 140 (2006).
[19] A. Kovács, K. Sato, and Y. Hirotsu, IEEE Trans. Magn. **43**, 3097 (2007).
[20] J. M. Howe, A. R. S. Gautam, K. Chatterjee, and F. Phillipp, Acta Mater. **55**, 2159 (2007).